Control of an Industrial Dual-arm Robot in a Narrow Space where Human Workers are Familiar with

Taeyong Choi[a], Hyunmin Do[b], Donil Park and Jinho Kyungk

Department of Robotics and Mechatronics, Korea Institute of Machinery and Materials, 156 Gajeongbuk-ro,
Yuseong-gu, Daejeon, South Korea

Keywords: Dual-arm Robot, Redundant Robot Control, Manufacturing with Robot.

Abstract: The industrial dual-arm robot is being developed. The developed industrial dual-arm robot aim to work with human workers or to work instead of human workers. Redundancy by high degree of freedom caused by arm and waist make robot movement difficult in the narrow space for human workers. Robot arms would take unexpected posture without proper redundant control method. In particular elbows can cause hazard situation by colliding with the environment or body of robot. Here novel method to control robot elbows is introduced. It shows good performance without loss of the position precision of end-effectors. Also it does not require high computing power, which make it useful for practical robot control. The proposed method is confirmed by the simulation.

1 INTRODUCTION

Robotic manufacturing is a significant technology to meet social needs. Population aging and decrease of working age population are critical social issues in the advanced country. In the advanced countries human workers are reluctant to do repetitive physical work. Many production lines can be replaced by robotic manufacturing with the current robotic technology. Industrial robot systems have been widely used for manufacturing such as laser welding, transfer and many repetitive processes.

However assembly works is still rely on human beings. Assembly works is fundamental process in the IT products production such as cellular phone, laptop and etc.. It is also true that manufacturing the trendy product such as cellular phone, automobile, food and clothes is possible only by human workers currently. The manufacturing system for the small quantity and batch production is significantly difficult with the automation equipment. Many researchers have studied robotic manufacturing systems. (Hayakawa et al., 1998) employed a manipulator to grasp the component parts during the assembly process. These improved the assembly cell only in the physical support aspect. (Kruger et al., 2009) introduced the examples of human-machine cooperation for assembly lines. However, there are no concreteness methods in it. (Morioka and Sakakibara, 2010) introduced new cell production assembly system with human-robot cooperation. However there have been no practical improvement yet.

Conventional industrial robot such as the serial robot has only one arm. In case of serial robot, 6 degrees of freedom (DOF) commonly used to position the end-effector of robot to exact position with orientation. However, they have limitation to replace human worker because of their low DOF and one arm structure. Human has many DOF including redundant joints to be flexible for the complex work. Dual-arms cooperate to handle more complex and handful object.

Recently, companies and researchers are trying to develop novel manufacturing system with the industrial dual-arm robot (IDAR). IDARs such as the motoman of (Yaskawa, 2019), the yumi of (ABB, 2019) and the others of (Smith et al., 2012), are becoming upcoming technology for robotic manufacturing. IDAR is distinguished with the humanoid-like service robots by the factors of traditional industrial robot performance indexes including high precision, high velocity and accessories of a teaching pendant and control box.

Most of IDARs have redundant joints unlike 6 DOF conventional manipulator. Some of them has DOF more than 6 at each arms. Some of them have

[a] https://orcid.org/0000-0002-4752-849X
[b] https://orcid.org/0000-0002-2588-0572

339

waists causing redundancy. These redundancy can be utilized to get proper posture during works(Colomé and Torras, 2012). The redundancy makes troubles without proper control. Conventional industrial robots are commanded at the joint space or cartesian space by its own teaching pendant. When it is run at cartesian space unconstrained redundant joints can collide with environments or by themselves. For example robot can be placed in narrow space with pre-installed equipments.

In this paper, we will introduce the fast and efficient dual-arm robot redundant posture method. There are some assumptions. We will not talk about how to detect collisions, and how to avoid collisions between the body and the environment. Collision detection algorithms requires much computing power to be used in real-time control for the industrial robots.

2 THE DEVELOPED ROBOTIC MANUFACTURING

Robotic manufacturing for IT product assembly and packaging is designed like fig. 1. Actually, this pilot line is for cellular phone packaging. Currently, IT products such as mobile phone and TV are made by human, who works all day at the designated area with standing. Their work is repetitive. Robot, specifically, IDAR which have functions like human can be a proper substitution for this kinds of tedious and repetitive works. In our scenario, two or three IDAR cooperate to assemble cellular phones. Also, they can pack cellular phones. Because IDAR have two arms like human, then can manage objects as human do without additional machines. (Do et al., 2016) describes details of robotic factory.

A IDAR, ambidextrous industrial robot (AMIRO) of fig. 2, was developed. Its physical properties are described in table 1. It has 7 DOF in each arms and 2 DOF in waist. Arm length is measured from shoulder to write. Body length is measured from shoulder to waist pitch axis. The payload to weight ratio will be at least 1/2. All actuators and force-torque sensors are communicated by the EtherCAT protocol. EtherCAT is communication standard introduced by BECKHOFF inc.. It uses the conventional local area network (LAN) physical layer and hardware, so user does not need to add any special equipment. In our robot, hollow axis actuators and sensors are used and all signals connected through the hole.

Figure 1: The developed robotic manufacturing system to pack cellular phones with multiple industrial dual-arm robots.
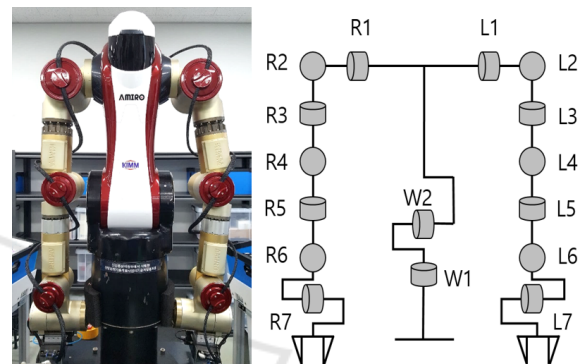

Figure 2: The developed industrial dual-arm robot, 'AMIRO'.

Table 1: Dual-arm robot specification.

	DOF	Weight(Kg)	Length(mm)
Right arm	7	14.5	700
Left arm	7	14.5	700
Waist	2	14.0(Body)	570

3 REDUNDANCY CONTROL IN THE INDUSTRIAL DUAL-ARM ROBOT

3.1 Basic Idea

In robotic factory it is natural that IDARs cooperate with human workers or work alone in human-familiar environment. In this reason large room for the motion to be easy is not provided for IDARs. Conventional industrial robots are with fences that make a enough room only for the robot. IDARs should consider collision against to environment. To meet those problems IDAR need to increase DOF like human-beings. The main advantage of redundancy is to be able to perform secondary tasks and/or to choose which solution suits us best. To this purpose, an optimization

criterion can be set to find, within the set of IK solutions, the one that performs best according to the criterion. The most common procedure is to project a gradient of a secondary task into the kernel of the Jacobian matrix, in order not to affect much the position error. With the redundancy IDAR can do secondary tasks such as collision avoidance, acquiring joint motion margin, natural motion and so on.

There were many previous researches to control redundant manipulators. 'arm angle' is utilized to decide redundant arm posture in (Shimizu et al., 2008; Seraji and Bon, 1999). In those 'arm angle' was defined as angle between the plane configured by upper and lower arm and ground. 'arm angle' can not be defined for the dual-arm robot. Shoulder, those are static as base position of each arm in 'arm angle' approach, moves in IDAR. In case of IDAR collision avoidance with environments is possible with complex algorithms. However those method can not be run in the real robot control due to heavy computing power.

To make these problem simple a novel control method is proposed, in which elbows are contracted to the critical points (CP). CP can be determined as temporary positions to constrain the motion. CP_R and CP_L are shown in the fig. 3 for each right and left arm. Virtual springs are positioned between CP_R and EB_R and between CP_L and EB_L. EB_R and EB_L are the elbow of right arm and left arm. Nominal length of virtual springs set to zero, so virtual springs always contract elbows by spring forces.
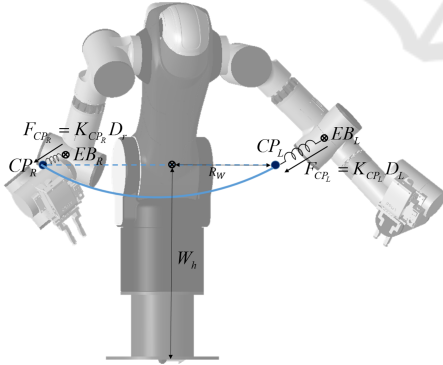

Figure 3: Conceptual view of the proposed method [front view]. Virtual springs are positioned between CP and elbows (EB).

3.2 Virtual Spring based Elbow Control

It is noticeable that dynamics control scheme is not used but gravity compensation because of lack of real dynamic parameters in the proposed method. In this reason virtual spring's contraction forces does not given to directly control laws. It is melted into
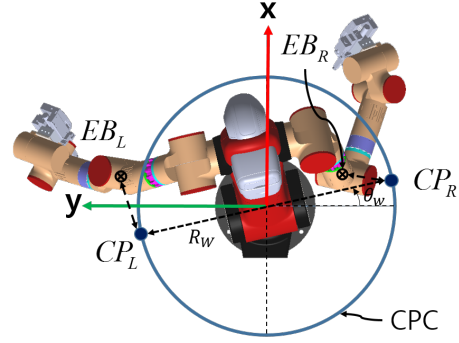

Figure 4: Conceptual view of the proposed method [top view].

inverse kinematics (IK) solving problem. Although there exists many methods to solve IK problem, the most popular way is to use closed loop inverse kinematics (CLIK) algorithms, a first order jacobian matrix is computed, which maps joint velocities into task space velocities, and inverted to map the task space error into a joint command difference which is likely to reduce the task space error. Joint command is updated with (1) and (2). To penalize singular points the damped least square method is used like (3). Gradient projection in (4) is used to decide redundant joint values.

$$\theta_d = \theta_s + \dot{\theta}_d \tag{1}$$

$$\dot{\theta}_d = \dot{\theta}_p + \dot{\theta}_n \tag{2}$$

$$\dot{\theta}_p = (J_e^T J_e + \lambda^2 I)^{-1} J_e^T \dot{x}^d \tag{3}$$

$$\dot{\theta}_n = (I - J_e^\dagger J_e)\nu \tag{4}$$

where θ_d, θ_s, $\dot{\theta}_p$ and $\dot{\theta}_n$ are a joint command, a joint state, a joint command update from damped least square and a joint command update in jacobian null space for gradient projection. Jacobian pseudo inverse $J_e^\dagger$ is described by (5) with a non-square jacobian matrix J_e and a damping parameter λ. ν is a gradient.

$$J_e^\dagger = (J_e^T J_e + \lambda^2 I)^{-1} J_e^T \tag{5}$$

A cost value Φ is defined like (6) where χ_R and χ_L are defined as power of contraction force between CP_R and EB_R, CP_L and EB_L, in each arm for convenience. Details are described in (7) and (8).

$$\Phi = \chi_R + \chi_L \tag{6}$$

$$\chi_R = F_{CP_R}{}^2 \tag{7}$$

$$\chi_L = F_{CP_L}{}^2 \tag{8}$$

Contraction forces F_{CP_R} and F_{CP_L} by virtual springs are defined in (9) and (10).

$$F_{CP_R} = K_{CP_R} D_R = K_{CP_R}||EB_R - CP_R|| \tag{9}$$

$$F_{CP_L} = K_{CP_L} D_L = K_{CP_L}||EB_L - CP_L|| \tag{10}$$

where K_{CP_R} and K_{CP_L} are spring constants, D_R and D_L are spring lengths, EB_R and EB_L are elbow positions, CP_R and CP_L are critical positions, in other words, spring positions for each right and left virtual springs. Distances of D_R and D_L are defined as (11) and (12).

$$D_R = ||EB_R - CP_R|| \qquad (11)$$

$$D_L = ||EB_L - CP_L|| \qquad (12)$$

The gradient is defined as (13) to reduce cost while robot working.

$$\nu = -\nabla\Phi = -\frac{\partial\Phi}{\partial\theta} = -[\frac{\partial\Phi}{\partial\theta_1}, \frac{\partial\Phi}{\partial\theta_2}, ..., \frac{\partial\Phi}{\partial\theta_n}]^T \quad (13)$$

where θ_i are each joint states in n DOF robot for $i = \{1, 2, ..., n\}$. Gradient is linearly decomposed as :

$$\nu = -(\frac{\partial\chi_R}{\partial\theta} + \frac{\partial\chi_L}{\partial\theta}) \qquad (14)$$

Finally gradient becomes:

$$\nu = -[\frac{\partial\chi_R}{\partial\theta_1} + \frac{\partial\chi_L}{\partial\theta_1}, \frac{\partial\chi_R}{\partial\theta_2} + \frac{\partial\chi_L}{\partial\theta_2}, ..., \frac{\partial\chi_R}{\partial\theta_n} + \frac{\partial\chi_L}{\partial\theta_n}]^T$$
$$(15)$$

EB_R, EB_L, CP_R and CP_L are defined as (16), (17), (18) and (19).

$$EB_R = (EB_{R_x}, EB_{R_y}, EB_{R_z}) \qquad (16)$$

$$EB_L = (EB_{L_x}, EB_{L_y}, EB_{L_z}) \qquad (17)$$

$$CP_R = (CP_{R_x}, CP_{R_y}, CP_{R_z}) \qquad (18)$$

$$CP_L = (CP_{L_x}, CP_{L_y}, CP_{L_z}) \qquad (19)$$

χ_R and χ_L from (7) and (8) are expanded to (20) and (21) with (11)$\sim$(19).

$$\chi_R = K_{CP_R}{}^2(D_{R_x}{}^2 + D_{R_y}{}^2 + D_{R_z}{}^2) \qquad (20)$$

$$\chi_L = K_{CP_L}{}^2(D_{L_x}{}^2 + D_{L_y}{}^2 + D_{L_z}{}^2) \qquad (21)$$

where D_{R_x}, D_{R_y}, D_{R_z}, D_{L_x}, D_{L_y} and D_{L_z} are followings:

$$D_{R_x} = EB_{R_x} - CP_{R_x} \qquad (22)$$

$$D_{R_y} = EB_{R_y} - CP_{R_y} \qquad (23)$$

$$D_{R_z} = EB_{R_z} - CP_{R_z} \qquad (24)$$

$$D_{L_x} = EB_{L_x} - CP_{L_x} \qquad (25)$$

$$D_{L_y} = EB_{L_y} - CP_{L_y} \qquad (26)$$

$$D_{L_z} = EB_{L_z} - CP_{L_z} \qquad (27)$$

Each terms of $\frac{\partial\chi_R}{\partial\theta_i}$ and $\frac{\partial\chi_L}{\partial\theta_i}$ in (15) are more described in detail as (28) and (29) for $i = 1, 2, ..., n$ with (20) and (21).

$$\frac{\partial\chi_R}{\partial\theta_i} = 2K_{CP_R}{}^2(D_{R_x}\frac{\partial D_{R_x}}{\partial\theta_i} + D_{R_y}\frac{\partial D_{R_x}}{\partial\theta_i} + D_{R_z}\frac{\partial D_{R_x}}{\partial\theta_i})$$
$$(28)$$

$$\frac{\partial\chi_L}{\partial\theta_i} = 2K_{CP_L}{}^2(D_{L_x}\frac{\partial D_{L_x}}{\partial\theta_i} + D_{L_y}\frac{\partial D_{L_x}}{\partial\theta_i} + D_{L_z}\frac{\partial D_{L_x}}{\partial\theta_i})$$
$$(29)$$

Partial differential of (22)$\sim$(27) can be determined with the jacobians between origin to elbows; $J_{R_{EB}}$ and $J_{L_{EB}}$. Those jacobians can be achieved easily with additional light calculations.

$$\frac{\partial D_{R_x}}{\partial\theta_i} = J_{R_{EB}}(1, i) - \frac{\partial CP_{R_x}}{\partial q_i} \qquad (30)$$

$$\frac{\partial D_{R_y}}{\partial\theta_i} = J_{R_{EB}}(2, i) - \frac{\partial CP_{R_y}}{\partial q_i} \qquad (31)$$

$$\frac{\partial D_{R_z}}{\partial\theta_i} = J_{R_{EB}}(3, i) - \frac{\partial CP_{R_z}}{\partial q_i} \qquad (32)$$

$$\frac{\partial D_{L_x}}{\partial\theta_i} = J_{L_{EB}}(1, i) - \frac{\partial CP_{L_x}}{\partial q_i} \qquad (33)$$

$$\frac{\partial D_{L_y}}{\partial\theta_i} = J_{L_{EB}}(2, i) - \frac{\partial CP_{L_y}}{\partial q_i} \qquad (34)$$

$$\frac{\partial D_{L_z}}{\partial\theta_i} = J_{L_{EB}}(3, i) - \frac{\partial CP_{L_z}}{\partial q_i} \qquad (35)$$

where $J_{R_{EB}}(p, q)$ and $J_{L_{EB}}(p, q)$ are elements of jacobian matrix at pth row and qth column for each elbow of right and left arms.

4 SIMULATION STUDY

A simulation is conducted to show the effectiveness of the proposed method. A WIDAR positioned instead of a human-workers. CPs are determined as described in section 4. User parameters of R_w and W_h are set as $0.3m$ and $0.57m$ from the dimension of AMIRO.

Fig. 5a shows dual-arm motion with the conventional method, in other words there is no constraint on elbow positions. Fig. 5b is with the proposed method. Elbows are contracted to the CPs on the CPC. Circles of A and A' are right end-effector motion for each method, and they are exactly same. Circles of B and B' are left end-effector motion, and they are same too. Fig. 6a and 6b show trajectories of end effectors. Trajectories of the conventional method and the proposed method are exactly same because both use same damping variables. The proposed method use null space to get redundant motions of elbows. However elbow motion is quite different. In the conventional method the motion of elbow is stick to minimum velocity criteria without constraints. That causes the smallest movements of elbows to reach a goal. In the proposed method elbows are forced to go to the determined CPs. Fig. 7 shows trails of elbow positions in three dimensional (3D) space. Fig. 8, 9 and 10 show same trails in each xy, xz and yz plane.

Contraction force between CP_R and EB_R is plotted in Fig. 11a. Contraction force between CP_L and EB_L is plotted in fig. 11b. In the proposed method contraction forces are decreased if it can, that means the
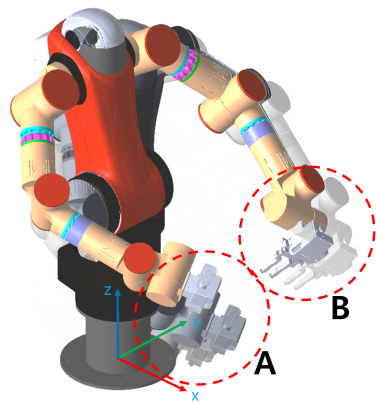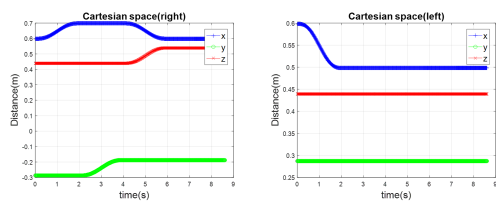
(a) Dual-arm robot motion with Moore-Penrose method.
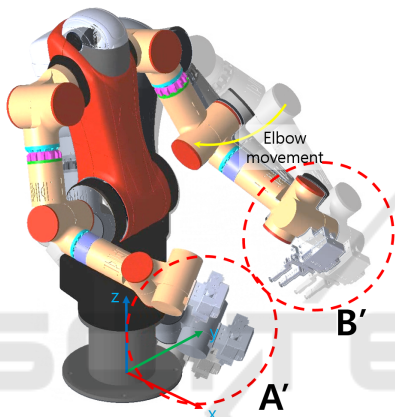
(b) Dual-arm robot motion with the proposed method.

Figure 5: Comparison of dual-arm robot motions.

(a) Right.   (b) Left.

Figure 6: The end-effector trajectory.

distances between *CP*s and *EB*s are reduced as short as possible. In fig. 11a contraction force increase for a while after 1sec. It is because elbow motions run without effect on end-effector positions.

5 CONCLUSION

Dual-arm robot is a novel industrial robot with two arms. It has high redundancy in motion inevitably.In
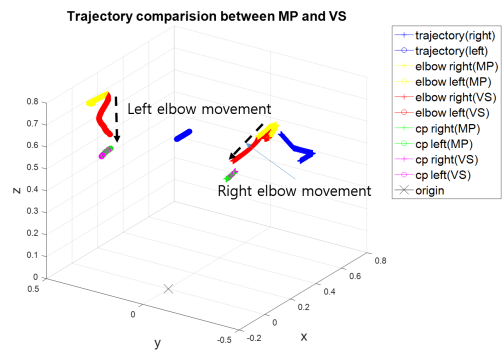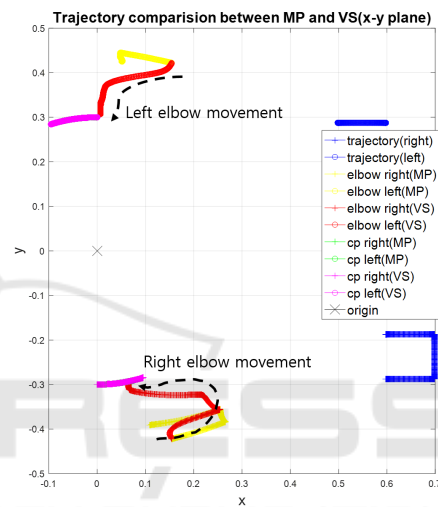

Figure 7: Trajectories(elbow, CP, end-effector).

Figure 8: Trajectories in *xy* plane(elbow, CP, end-effector).
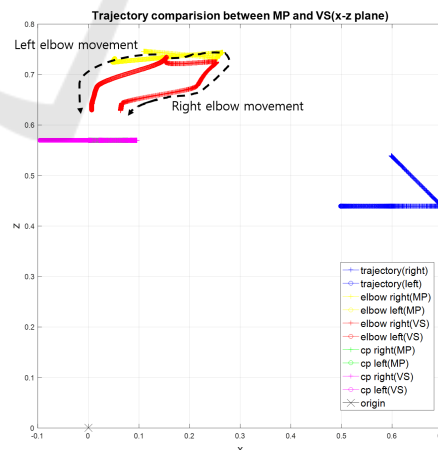

Figure 9: Trajectories in *xz* plane(elbow, CP, end-effector).

practical both arms cause undesired motions including colliding against to environments without proper control. To resolve this problem a novel control method is proposed in this paper. The proposed method try to limit elbows motion to be contracted to
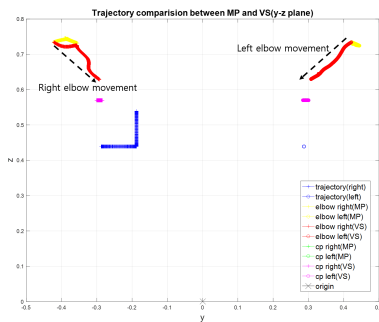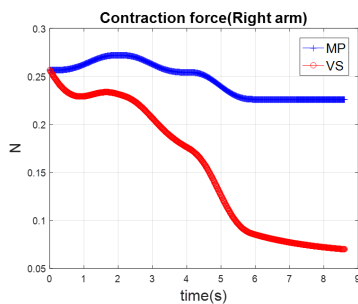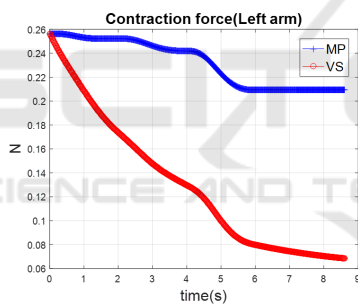
Figure 10: Trajectories in *yz* plane(elbow, CP, end-effector).

(a) Contraction force(right).

(b) Contraction force(left).

Figure 11: Contraction force.

the contraction points via virtual springs algorithm. Contraction points are decided to mimic the motion of human worker. In simulation studies the proposed algorithm induced the desired motion to control redundant dual-arm robot.

REFERENCES

ABB (2019). How human-robot collaboration is driving a manufacturing revolution.

Colomé, A. and Torras, C. (2012). Redundant inverse kinematics: Experimental comparative review and two enhancements. In *Intelligent Robots and Systems (IROS), 2012 IEEE/RSJ International Conference on*, pages 5333–5340. IEEE.

Do, H. M., Choi, T.-Y., and Kyung, J. H. (2016). Au-tomation of cell production system for cellular phones using dual-arm robots. *The International Journal of Advanced Manufacturing Technology*, 83(5-8):1349–1360.

Hayakawa, Y., Kitagishi, I., and Sugano, S. (1998). Human intention based physical support robot in assembling work. In *Proceedings of IROS*, pages 930–935.

Kruger, J., Lien, T., and Verl, A. (2009). Cooperation of human and machines in assembly lines. *CIRP Annals-Manufacturing Technology*, 58(2):628–646.

Morioka, M. and Sakakibara, S. (2010). A new cell production assembly system with human-robot cooperation. *CIRP Annals-Manufacturing Technology*, 59(1):9–12.

Seraji, H. and Bon, B. (1999). Real-time collision avoidance for position-controlled manipulators. *Robotics and Automation, IEEE Transactions on*, 15(4):670–677.

Shimizu, M., Kakuya, H., Yoon, W.-K., Kitagaki, K., and Kosuge, K. (2008). Analytical inverse kinematic computation for 7-dof redundant manipulators with joint limits and its application to redundancy resolution. *Robotics, IEEE Transactions on*, 24(5):1131–1142.

Smith, C., Karayiannidis, Y., Nalpantidis, L., Gratal, X., Qi, P., Dimarogonas, D. V., and Kragic, D. (2012). Dual arm manipulation—a survey. *Robotics and Autonomous systems*, 60(10):1340–1353.

Yaskawa (2019). Slim dual-arm robot.